American Mineralogist, Volume 95, pages 1125–1131, 2010

Resonant X-ray emission study of the lower-mantle ferropericlase at high pressures

JUNG-FU LIN,[1,*] ZHU MAO,[1] IGNACE JARRIGE,[2] YUMING XIAO,[3] PAUL CHOW,[3] TAKUO OKUCHI,[4] NOZOMU HIRAOKA,[5] AND STEVEN D. JACOBSEN[6]

[1]Department of Geological Sciences, Jackson School of Geosciences, The University of Texas at Austin, Austin, Texas 78712, U.S.A.
[2]Synchrotron Radiation Research Unit, Japan Atomic Energy Agency, Hyogo 679-5148, Japan
[3]HPCAT, Geophysical Laboratory, Carnegie Institution of Washington, Argonne, Illinois 60439, U.S.A.
[4]Institute for Study of the Earth's Interior, Okayama University, Yamada 827, Misasa, Tottori 682-0193, Japan
[5]National Synchrotron Radiation Research Center, Hsinchu 30077, Taiwan
[6]Department of Earth and Planetary Sciences, Northwestern University, Evanston, Illinois 60208, U.S.A.

ABSTRACT

Electronic states of iron in Earth's mantle minerals including ferropericlase, silicate perovskite, and post-perovskite have been previously investigated at high pressures and/or temperatures using various experimental techniques, including X-ray emission and Mössbauer spectroscopies. Although such methods have been used to infer changes in the electronic spin and valence states of iron in lower mantle minerals, they do not directly probe the 3*d* electronic states quantitatively. Here we use 1*s*2*p* resonant X-ray emission spectroscopy (RXES) at the Fe *K* pre-edge to directly probe and assess the 3*d* electronic states and the crystal-field splittings of Fe^{2+} in the lower-mantle ferropericlase [$(Mg_{0.75},Fe_{0.25})O$] at pressures up to 90 GPa. The pre-edge features from X-ray absorption spectroscopy in the partial fluorescence yield (PFY-XAS) and RXES results explicitly show three excited states for high-spin Fe^{2+} (a lower-energy $^4T_{1g}$ state, a $^4T_{2g}$ state, and a higher-energy $^4T_{1g}$ state) and a single ^2E_g state for low-spin Fe^{2+}, attributed to the $(t_{2g})^0(e_g)^3$ excited configuration. This latter feature begins to appear at 48 GPa and grows with pressure, while the peaks related to high-spin Fe^{2+} vanish above 80 GPa. The observed pre-edge features are consistent with purely quadrupolar transitions resulting from the centrosymmetric character of the Fe^{2+} site. The *K* pre-edge RXES spectra at the incident energy of 7112 eV, which are similar to the Fe *L*-edge spectra, are also used successfully to quantitatively obtain consistent results on the spin transition of Fe^{2+} in ferropericlase under high pressures. Owing to the superior sensitivity of the RXES technique, the observed electronic states and their energy separations provide direct information on the local electronic structures and crystal-field splitting energies of the 3*d* electronic shells of Fe^{2+} in ferropericlase at relevant pressures of the Earth's lower mantle.

Keywords: Ferropericlase, diamond anvil cell, spin transition, resonant X-ray emission spectroscopy, partial fluorescence yield, high pressures

INTRODUCTION

Electronic states of iron, including total spin momentum and valence charge, have been studied extensively at high pressures in lower-mantle ferropericlase, silicate perovskite, and post-perovskite, owing to their influence on a range of physical properties relevant to understanding the state and dynamics of the Earth's deep interior (e.g., Badro et al. 2003, 2004; Catalli et al. 2010; Grocholski et al. 2009; Jackson et al. 2005; Lin et al. 2005, 2008; Lin and Tsuchiya 2008; McCammon et al. 2008; Persson et al. 2006; Tsuchiya et al. 2006). In particular, a high-spin to low-spin transition of Fe^{2+} has been reported in ferropericlase [(Mg,Fe)O] at high pressures using Mössbauer spectroscopy (Speziale et al. 2005; Gavriliuk et al. 2006; Kantor et al. 2006; Lin et al. 2006, 2009; Lyubutin et al. 2009), X-ray emission spectroscopy (XES) (Badro et al. 2003; Lin et al. 2005, 2007), and optical absorption spectroscopy (Goncharov et al. 2006; Keppler et al. 2007). These techniques have long played important and complementary roles in studying the electronic structures of planetary materials in extreme environments.

Although many experimental techniques allow inference of changes in spin and valence states by measuring electrical, optical, vibrational, magnetic, or structural properties, few directly probe the 3*d* electronic states quantitatively (e.g., Lin and Tsuchiya 2008). For example, XES and Mössbauer spectroscopy probe processes occurring in the inner electronic shell (in XES) or in the nuclei of iron ions (in Mössbauer) as indicators of the electronic spin transitions that occur in the outermost 3*d* orbitals of the iron ions (Maddock 1997; Vankó et al. 2006). Mössbauer spectroscopy has been widely used to investigate spin transitions of iron in lower-mantle minerals owing to its sensitivity to the hyperfine parameters of iron nuclei, which can reflect the redistribution of 3*d* electrons across the spin transitions (Maddock 1997). In XES, the Fe *K*β′ satellite peak arising from the 3*p*-3*d* electronic exchange interaction is sensitive to the local magnetic moment of the dilute iron-containing minerals, but it does not necessarily distinguish between various valence states or coordination numbers. Furthermore, the intensity of the *K*β′ satellite peak is a complex function of many factors, from which the

* E-mail: afu@jsg.utexas.edu

average spin number might be extracted (Vankó et al. 2006).

Recent advances in synchrotron X-ray spectroscopic techniques have stimulated application of X-ray absorption spectroscopy (XAS) and/or resonant X-ray emission spectroscopy [RXES; or called resonant inelastic X-ray scattering (RIXS)] as new probes to assess the 3*d* electronic states of iron-containing compounds (e.g., Caliebe et al. 1998; Wilke et al. 2001; Rueff et al. 2004; Vankó et al. 2006; Narygina et al. 2009). As an example, a recent study of the Fe *K* pre-edges by XAS for a series of Fe-containing minerals showed that the pre-edge peak position and intensity distribution varied systematically with spin state, oxidation state, geometry, and bridging ligation (e.g., Wilke et al. 2001). However, intrinsic limitations of XAS arise from the spectral resolution, which is ultimately limited by the 1*s* core-hole lifetime width of ~1.15 eV. Interpretation of XAS pre-edge spectra is further complicated in some cases by contributions of both dipolar and quadrupolar components (e.g., Caliebe et al. 1998; Rueff et al. 2004; Narygina et al. 2009).

Applied to the Fe *K* pre-edge of Fe-containing compounds, RXES has recently been shown to be a powerful probe of the unoccupied 3*d* electronic structure (e.g., Caliebe et al. 1998; Rueff et al. 2004), by virtue of the suppression of the core-hole lifetime broadening and the possibility to resonantly enhance specific intermediate states by properly tuning the excitation energy. Because the final state of the 1*s*2*p* RXES process, a core-hole in the 2*p* level, is identical to that of the *L*-edge absorption process, it is possible to obtain *L*-edge-like information even under constrained sample environments. The application of this technique to high-pressure science has, however, been limited so far by low count rates and the parasitic contamination from Fe impurities contained in Be gaskets. Those difficulties were overcome in the present study and we successfully conducted 1*s*2*p* RXES experiments at the Fe *K* pre-edge of ferropericlase [$(Mg_{0.75},Fe_{0.25})O$] under high pressure.

Ferropericlase contains mostly Fe^{2+} in the octahedrally coordinated local environment (O_h symmetry), which makes it an ideal candidate for this first high-pressure RXES case study on the electronic structures of the mantle minerals. We have measured the pre-edge features using both X-ray absorption spectroscopy in the partial fluorescence yield mode (PFY-XAS), the so-called lifetime removed XAS, and 1*s*2*p* RXES at pressures up to 90 GPa. Through systematic analyses of the data, the spin states and the crystal-field splitting energies of Fe^{2+} in ferropericlase are derived at relevant lower-mantle pressures.

Resonant X-ray emission spectroscopy

Here we briefly discuss the RXES process and the anticipated pre-edge features of the octahedrally coordinated Fe^{2+} in ferropericlase. For simplicity and clarity, the RXES process for the centrosymmetric Fe^{2+} site is explained as a two-step process within a mono-electronic picture (Fig. 1a) (e.g., Caliebe et al. 1998; Rueff et al. 2004; Vankó et al. 2006). Based on crystal-field theory (Burns 1985, 1993), the ground state of Fe^{2+} ($3d^6$) in the O_h ligand field consists of an electron hole configuration of $(t_{2g})^2(e_g)^2$ for the high-spin state and $(t_{2g})^0(e_g)^4$ for the low-spin state (where the superscripted number outside the parentheses represents the number of available electron holes) (Figs. 1b–1c). In the first step, a 1*s* electron is promoted to the $\underline{1s}3d^7$ or $\underline{1s}3d^6 4p^1$ intermediate state through quadrupolar and dipolar excitations (Fig. 1a) (the underlined electronic configurations are the hole states), respectively, that are primarily assigned to the pre-edge and white line spectral regions. In the second step, the final states are reached by decay of a 2*p* electron into the empty 1*s* state, leading to the $\underline{2p}3d^7$ or $\underline{2p}3d^6 4p^1$ configuration. We note that, in the present case, one expects the pre-edge features only stem from the quadrupolar transitions because of the centrosymmetric character of the O_h Fe^{2+} site in ferropericlase.

The octahedral ligand field around the Fe^{2+} ion results in the 3*d* orbital splitting into a t_{2g} and an e_g set (Burns 1985, 1993). The pre-edge feature would be dominated by four many-electron states (a lower-energy $^4T_{1g}$ state, a $^4T_{2g}$ state, a higher-energy $^4T_{1g}$ state, and $^4A_{2g}$) after removing degeneracy of the 3*d* orbitals (Griffith 1961; Westre et al. 1997). The $^5T_{2g}$ ground state of high-spin Fe^{2+} in an O_h ligand field has an electronic hole configuration of $(t_{2g})^2(e_g)^2$. For the high-spin state, promotion of an 1*s* electron into the 3*d* shell yields, therefore, one of the two possible excited hole configurations, $(t_{2g})^1(e_g)^2$ or $(t_{2g})^2(e_g)^1$ (Fig. 1b). The $(t_{2g})^1(e_g)^2$ configuration gives rise to a $^4T_{1g}$ state, while the $(t_{2g})^2(e_g)^1$ configuration results in a $^4T_{1g}$ and a $^4T_{2g}$ state (Griffith 1961; Westre et al. 1997). The high-spin $^4A_{2g}$ state originates from a two-electron excited hole configuration, $(t_{2g})^3$, and thus it will not contribute to the pre-edge region and cannot mix with any of the one-electron allowed states from the symmetry considerations.

The ground state of low-spin Fe^{2+} has an electronic hole configuration of $(t_{2g})^0(e_g)^4$. The only 1*s*→3*d* pre-edge feature for low-spin Fe^{2+} in the O_h site is the allowed electric quadrupole transition, with $(t_{2g})^0(e_g)^3$ being the only allowed excited hole configuration, which produces a ^2E_g excited many-electron state (Fig. 1c). Therefore, a high-spin to low-spin transition of Fe^{2+} in ferropericlase would manifest itself as a change from the three distinct peaks (a lower-energy $^4T_{1g}$ state, a $^4T_{2g}$ state, and a higher-energy $^4T_{1g}$ state) into the a single-peak (^2E_g state) in the pre-edge region (Fig. 1) (Westre et al. 1997).

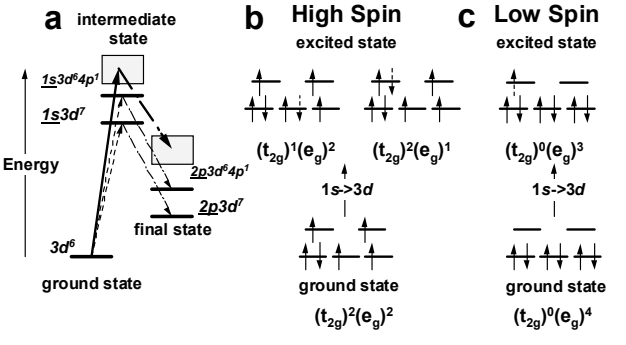

Figure 1. Schematic representation of 1*s*2*p* RXES transitions for octahedrally coordinated Fe^{2+} in ferropericlase at the Fe *K* pre-edge based on crystal field theory (after Caliebe et al. 1998; Rueff et al. 2004). (**a**) A two-step RXES transition process within a mono-electronic picture. The quadrupolar and dipolar transitions are indicated by thick and thin lines, respectively. (**b**) Ground and excited states of the octahedrally coordinated high-spin Fe^{2+}. (**c**) Ground and excited states of the octahedrally coordinated low-spin Fe^{2+}. The dashed arrows in **b** and **c** represent the excited electron.

EXPERIMENTAL METHODS

Single-crystal (with [100] platelet) or polycrystalline $(Mg_{0.75},Fe_{0.25})O$ samples were used for the high-pressure RXES experiments. Iron in our samples was predominantly present as ferrous iron (Fe^{2+}). The ferric iron (Fe^{3+}) of the samples was below the detection limit of Mössbauer spectroscopy, and magnetite (Fe_3O_4) was not detected by X-ray diffraction (Jacobsen et al. 2002; Lin et al. 2006), ensuring that the measured RXES features are exclusively contributed by the Fe^{2+} in ferropericlase. Ultrapure Be gaskets (IF-1 grade; Bruch Wellman, Electrofusion Products) of 2 mm in diameter and 250 μm thick were pre-drilled to fit the shape of the beveled diamond anvils of 150–300 μm in diameter or those of flat diamonds of 300 μm in diameter, and then pre-indented to ~25 μm thickness. The ultrapure Be gaskets contain less than 0.03% iron impurity, which is a factor of five less than that in the more commonly used I-220-H grade Be gaskets with ~0.15% iron impurity. Subsequently, a hole of 200 μm in diameter was drilled in the pre-indented area and filled with cubic BN to form a gasket insert (Lin et al. 2008). A hole of ~80 μm in diameter was then drilled and used as the sample chamber. Either a single-crystal or a pre-compressed disk of polycrystalline sample measuring ~70 μm in diameter and 15 μm in thickness was loaded into the sample chamber in a panoramic diamond anvil cell (DAC) (Fig. 2), along with heavy mineral oil (a mixture of heavy hydrocarbon from Fisher Scientific, product number: MX1560) as the pressure medium and a few small ruby spheres for pressure measurements (Mao et al. 1978). The use of the cubic BN gasket insert was critical in maintaining sufficient thickness of the sample chamber (Lin et al. 2008) and in almost completely suppressing parasitic signal from the iron impurities from the Be during the RXES experiments (Fig. 3). Optical Raman and X-ray diffraction analyses of the samples and mineral oil after the experiments did not reveal any chemical reaction. Pressures were also measured from the shift of the first-order Raman bands of the diamond anvil near the center and edge of the sample chamber (Akahama and Kawamura 2007) to evaluate pressure gradients across the sample, which were ~10% of the sample pressures.

Due to the substantial absorption of the incident X-ray near 7 keV by the diamond anvil (even with an only 800 μm thick perforated anvil), we have employed a tilted experimental geometry, which allowed the incident X-ray to access the sample chamber through the gap between the diamond anvils and the Be gasket. This permits minimum absorption of the incident X-ray by the Be gasket and the diamond anvils while permitting the RXES signal to exit the sample chamber through the Be gasket (Fig. 2). Furthermore, because the incident X-ray only penetrated a limited portion of the Be gasket, the background noise from the Fe impurities in the Be gasket was further reduced (Fig. 3). We note that the tilted geometry, however, resulted in sampling a much larger pressure gradient across the sample, which likely is the reason for the observed wide transition region (see Discussion section for further information).

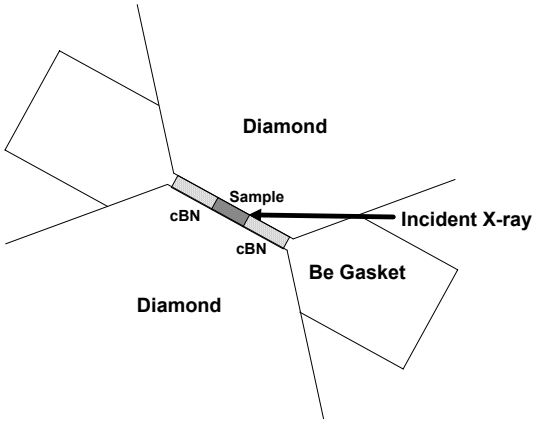

FIGURE 2. Schematic representation of the experimental geometry for the PFY-XAS and RXES experiments in a DAC. The DAC was tilted such that the horizontal incident X-ray beam entered the sample chamber at an angle of 28° from the Be gasket (through the gap between the Be gasket and the diamond anvils). The RXES signal exited the sample chamber through the Be gasket perpendicular to the incident X-ray. This experimental geometry significantly reduced the absorption of the incident X-ray and exiting signal by diamond anvils as well as the background noise from Fe impurities in the Be gasket.

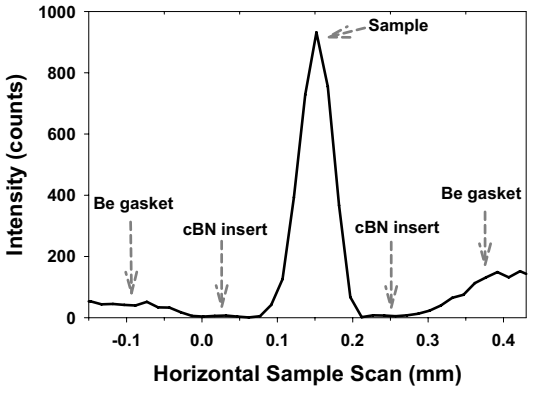

FIGURE 3. Representative scan of the sample chamber during the PFY-XAS and RXES experiments. This horizontal scan was perpendicular to the horizontal incident X-ray. The incident X-ray energy was set at 7200 eV in this scan, whereas the spectrometer energy was set at the peak of the Fe $K\alpha_1$ at 6403.84 eV. The scan was 10 s per step. The sample size was ~70 μm in diameter. The use of the BN gasket insert resulted in a nearly suppressed parasitic signal from the Fe impurities present in the Be gasket (which would have otherwise contributed up to 15–20% of the signal from the sample).

The PFY-XAS and RXES experiments were carried out at the HPCAT beamline of the Advanced Photon Source at high pressures. A monochromatic X-ray beam of around 7 keV with 1 eV bandwidth from a water-cooled diamond (111) double crystal monochromator was focused down to 30–70 μm in diameter at the sample position and used for the experiments. Spectra were recorded in the reflection mode using a Si (333) analyzer to monochromatize the scattered beam and an Amptek Si solid-state detector with a slit of ~100 μm in front of it. At the $K\alpha$ emission line energy, the associated Bragg angle was 67.847°. To reduce elastic scattering background, the angle between the incident X-ray beam and the sample-analyzer direction was set to 90°. Absolute energy of the system was calibrated using the Fe *K* absorption edge of an iron foil. The overall energy resolution of the systems was estimated to be 1.1 eV from the full-width at half maximum (FWHM) of the elastic peak measured at the Fe $K\alpha_1$ line energy, although measured spectral features can be well resolved within ~0.2 eV.

The PFY-XAS spectra were measured by setting the Bragg angle of the analyzer to the maximum of the $K\alpha_1$ emission line while scanning the incident energy (E_1) with a 0.2 eV step through the pre-edge between 7109 and 7117 eV (Fig. 4). Spectra with a total of 6000–10 000 counts at the maximum of the pre-edge peak were collected in a few hours at each pressure. The RXES spectra were measured at incident energies spanning the same pre-edge region with a 0.25 eV step, by scanning the analyzer Bragg angle while synchronously translating the detector. The measured transfer energy E_1-E_2 (where E_2 was the emission energy) was scanned between 704 and 713 eV with a 0.25 eV step (Figs. 5–6).

EXPERIMENTAL RESULTS AND DATA ANALYSES

The PFY-XAS and RXES pre-edge spectra of Fe^{2+} in ferropericlase were collected up to 90 GPa at ~10–20 GPa pressure intervals (Figs. 4–6). Three distinct spectral features can be well resolved up to ~37 GPa. An additional peak emerges at 48 GPa, the intensity of which increases with further pressure increase, until becoming a single, dominant spectral feature at 84 and 90 GPa.

To better understand the pressure dependence of the pre-edge spectral features, we have fitted the PFY-XAS data after removing the dipolar background contribution from the main edge and normalizing the resulting spectra by setting the total integrated area of the pre-edge region to unity. The pre-edge features were modeled by Voigt line shapes with the energy position, the

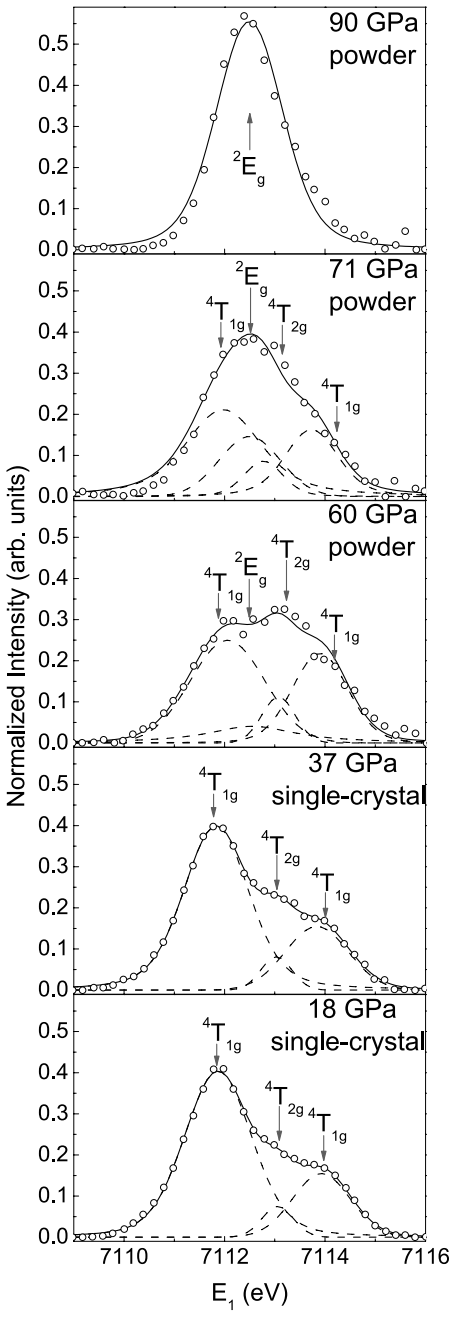

FIGURE 4. Representative pre-edge PFY-XAS spectra of ferropericlase [$(Mg_{0.75},Fe_{0.25})O$] at high pressures. Background contribution from the Fe *K* edge has been removed for clarity. The high-spin spectra were fitted to a three-peak model (a lower-energy $^4T_{1g}$, a $^4T_{2g}$, and a higher-energy $^4T_{1g}$), whereas the low-spin spectra were fitted to a single-peak ^2E_g model using Voigt peak shapes (Westre et al. 1997; Wilke et al. 2001) (see Fig. 1 for the transition processes). Circles = experimental data; solid lines = total fitted patterns; dashed lines = Voigt peaks for the high-spin and low-spin states. The ^2E_g state of the low-spin ferropericlase increased in intensity with increasing pressure. The relative intensity ratios of the three high-spin peaks for the single-crystal and polycrystalline samples, respectively, vary slightly because of the orientation and polarization-dependent factors, and were separately used to fit the spectra at high pressures using the intensity ratios under ambient conditions.

full-width at half maximum (FWHM), and the peak height as variables. Following previous pre-edge spectral assignments for the high-spin and low-spin Fe^{2+} complexes in the O_h geometry with three-peak and one-peak features, respectively (Westre et al. 1997), we modeled the spectra at ambient conditions with a three-peak model, which adequately reproduced the experimental spectral features up to 37 GPa. A fourth peak, thus a four-peak model, was needed to fit the spectra between 48 and 71 GPa, whereas a single Voigt function was utilized for the spectra at 84 and 90 GPa (Fig. 4). We found that fixing the relative intensity ratios of the three high-spin peaks (as derived from the spectrum at ambient conditions) has a negligible influence on the derived ratios of the high-spin and low-spin states. The RXES spectra measured at E_1 = 7112 eV at high pressures were also fitted using a linear combination of the RXES spectra measured at 18 and 84 GPa to evaluate the pressure-dependence ratio of the high-spin state (Fig. 6).

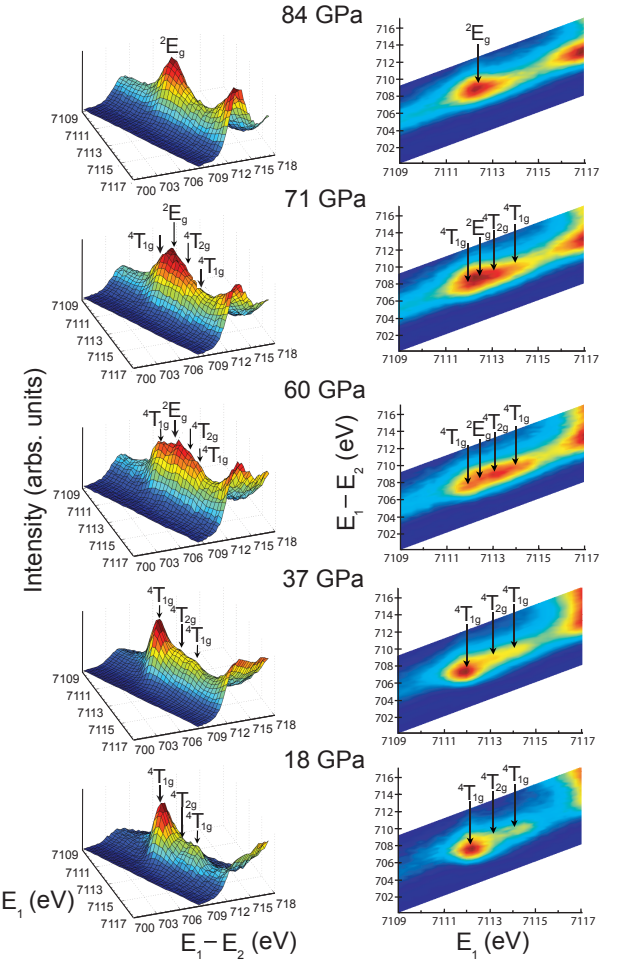

FIGURE 5. Representative pre-edge RXES spectra of ferropericlase [$(Mg_{0.75},Fe_{0.25})O$] at high pressures. (**a**) 3-dimentional plots; (**b**) contour plots. The spectra were normalized by setting the total integrated area to unity. E_1 = incident X-ray energy; E_2 = emitted photon energy; E_1-E_2 = transfer energy. Similar to Figure 4, the RXES spectra show the three high-spin excited states and one low-spin excited state.

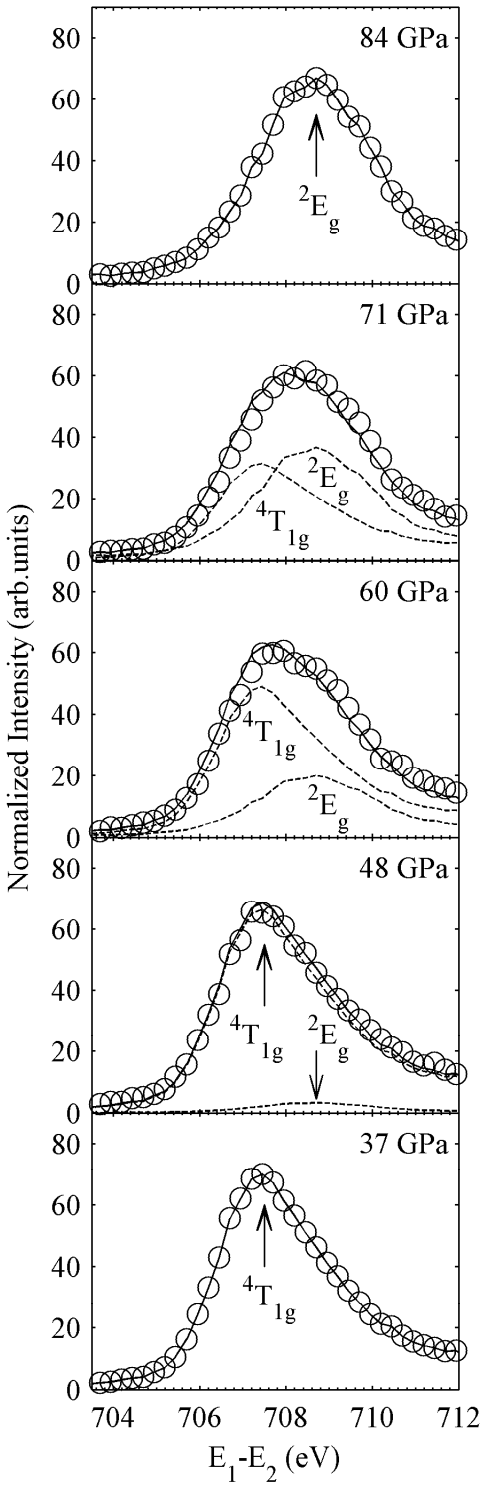

FIGURE 6. Representative RXES spectra of ferropericlase [$(Mg_{0.75},Fe_{0.25})O$] at E_1 = 7112 eV at high pressures (circles). The spectra were fitted (solid line) using a linear combination of the RXES spectra measured at 18 and 84 GPa (dashed lines). Since those spectra correspond respectively to pure high-spin $^4T_{1g}$ and pure low-spin ^2E_g, the pressure dependence of the high-spin state ratio can be directly derived from the pressure dependence of the ratio of $^4T_{1g}$ in the fit.

DISCUSSION

Based on a previous study (Westre et al. 1997), the pre-edge features in the three-peak model can be assigned to a lower-energy $^4T_{1g}$ state, a $^4T_{2g}$ state, and a higher-energy $^4T_{1g}$ state of the high-spin Fe^{2+}, with the lower-energy feature being more intense than the other two (Figs. 4–6). The lower-energy $^4T_{1g}$ peak arises from the $(t_{2g})^1(e_g)^2$ configuration of the excited high-spin state, whereas the $^4T_{2g}$ peak and the higher-energy $^4T_{1g}$ peak originate from the $(t_{2g})^2(e_g)^1$ state (Fig. 1b). The intensity of the $(t_{2g})^1(e_g)^2$-derived $^4T_{1g}$ final state is almost equal to the combined intensities of the $(t_{2g})^2(e_g)^1$-derived $^4T_{2g}$ and $^4T_{1g}$ states, consistent with the statistically weighted number of one-electron transitions from the ground state to the excited state. On the other hand, the peak centered at 7112.5 eV can be attributed to the ^2E_g excited many-electron state arising from the $(t_{2g})^0(e_g)^3$ configuration of the excited low-spin state (see Fig. 7 for relative energies of these states as a function of pressure). The occurrence of the ^2E_g state at ~48 GPa provides direct evidence for the high-spin to low-spin transition of Fe^{2+} in lower-mantle ferropericlase at high pressures.

The integrated area of the three high-spin related peaks decreases with increasing pressures between 48 and 71 GPa, and goes to zero at 84 and 90 GPa (Fig. 8). Since the integrated area represents the proportion of the high-spin state in ferropericlase, its disappearance and the concurrent appearance of the ^2E_g state signify the pressure-induced spin-pairing transition in ferropericlase. Derivation of the high-spin to the low-spin ratio using the

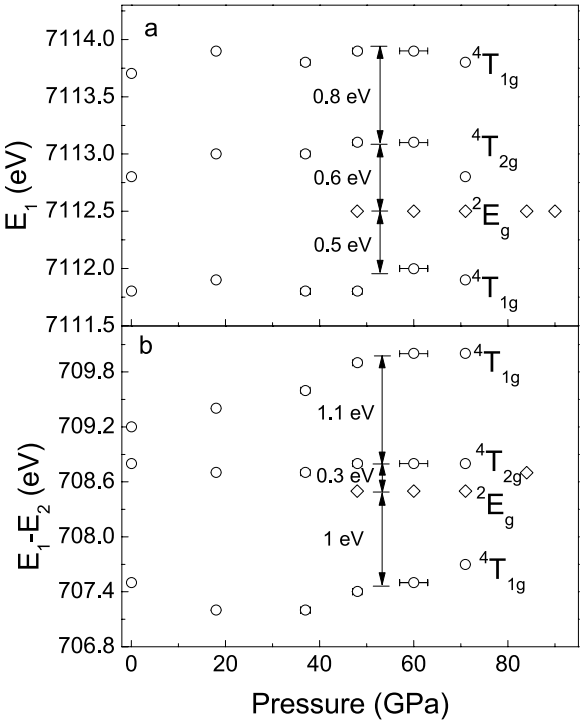

FIGURE 7. Measured peak energies of the excited states of Fe^{2+} in ferropericlase [$(Mg_{0.75},Fe_{0.25})O$] from the (**a**) PFY-XAS and (**b**) RXES spectra at high pressures. Energy shift between the different high-spin and low-spin states are indicated.

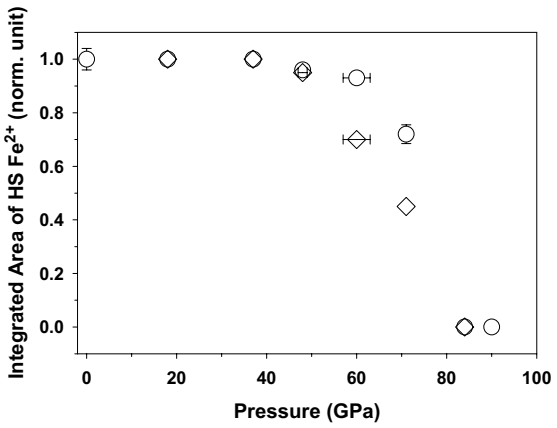

FIGURE 8. Integrated area of the high-spin Fe^{2+} in ferropericlase as a function of pressures. Open circles: PFY-XAS results (see Fig. 4); open diamonds: RXES results (see Fig. 6). These values derived from PFY-XAS and RXES spectra decrease with increasing pressure between 48 and 71 GPa, consistent with the transition to the low-spin state. Errors on the pressures were estimated from pressures measured from the ruby pressure calibrant before and after measurements.

RXES spectra measured at E_1 = 7112 eV at high pressures is consistent with the PFY-XAS results (Fig. 8).

Compared with the previous studies using synchrotron Mössbauer and Fe XES spectroscopies (Badro et al. 2003; Lin et al. 2005, 2007, 2009; Speziale et al. 2005; Gavriliuk et al. 2006; Kantor et al. 2006; Lin and Tsuchiya 2008), our results show a broader spin transition zone than X-ray emission studies (Lin et al. 2007, 2009) but a narrower transition than Mössbauer studies (Kantor et al. 2006). The discrepancy in these results may arise from different experimental conditions, such as the sample size, thickness, hydrostaticity in the sample chamber, and the beamsize of the X-ray source. In our experiments, relatively large pressure gradients of ~10% in our tilted geometry across the sample likely resulted in the observation of a broader transition region and may account for some of the discrepancy with previous studies. Although our studies here show that RXES has superior sensitivity to the detection of the electronic states of Fe^{2+} in ferropericlase at relevant pressures of the Earth's lower mantle, reconciling the width of the spin transition will require probing a smaller sample along the X-ray beam in a DAC.

The energy positions and separations of the observed high-spin and low-spin states provide direct experimental information to evaluate the unoccupied 3*d* electronic structure of Fe^{2+} in the lower-mantle ferropericlase (Fig. 7). Near the onset of the low-spin state at 48 GPa, the lower-energy $^4T_{1g}$ state is separated from the $^4T_{2g}$ state and from the high-energy $^4T_{1g}$ state by ~1.1 and 1.9 eV in E_1, respectively (Fig. 7). The low-spin ^2E_g state is about 0.5 eV higher than the lower-energy, high-spin $^4T_{1g}$ state, while lower than the other two high-spin states by 0.6 and 1.4 eV, respectively.

Consistent pressure dependences of the high-spin state ratio have been derived both from the PFY-XAS spectrum and the RXES spectrum at E_1 = 7112 eV. This is worth noticing since these spectra yield, respectively, *K*-edge and *L*-edge-like information. The good agreement between the two therefore confirms that both edges can be used successfully to infer semi-quantitative information about the spin state. Owing to the large Coulomb interaction between the 2*p* and 3*d* levels, the *L* edge offers a higher sensitivity to charge and spin states than the *K* edge (Cressey et al. 1993). This is confirmed here with the E_1 = 7112 eV RXES spectrum where each spin state yields a single feature split by 1 eV (Fig. 6). Although *L*-edge spectroscopy cannot be performed under high pressure because of the low photon energy, our study shows that spectra nearly similar to *L*-edge ones (Cartier dit Moulin et al. 1992; Briois et al. 1995; Huse et al. 2009) can be obtained using the RXES at the Fe *K* edge.

Our PFY-XAS and RXES results provide direct and consistent evidence for the pressure-induced spin-pairing transition of Fe^{2+} in lower-mantle ferropericlase. With this sensitive technique, our results show that the spin transition occurs between 48 and 84 GPa, which is relatively higher than most of the previous studies. Future studies having a smaller sample under quasi-hydrostatic pressures would help in resolving discrepancy in the width of the spin transition. This study also implies that the PFY-XAS spectra, which correspond to a diagonal sampling of the RXES surface as shown in Figure 5, can serve as a useful tool to monitor the variations of the electronic configuration. We note that the PFY-XAS spectra have higher energy resolution and better separation of spectral features than the conventional XAS (e.g., Narygina et al. 2009). On the other hand, the RXES spectra at the E_1 = 7112 eV, with spectra features similar to the Fe *L*-edge, yield consistent results on the spin transition, thus rendering the analysis easier and, to some extent, more reliable than the *K*-edge-like PFY-XAS spectrum which suffer from more complex multiplet structures (Figs. 4 and 6).

The PFY-XAS and RXES techniques over the pre-edge region thus provide direct means to probe the 3*d* electronic structures and the crystal-field splittings of planetary materials at high pressures. By taking advantage of the sharpening effect of the RXES process, future studies using better energy resolution, i.e., 0.25 eV, and smaller X-ray beam size would help to address some outstanding questions on the 3*d* electronic structures of iron in more complex systems such as the lower-mantle silicate perovskite and post-perovskite (e.g., Lin et al. 2008b; McCammon et al. 2008).

AKNOWLEDGMENTS

High-pressure experiments were performed at HPCAT of the Advanced Photon Source (APS) at the Argonne National Laboratory (ANL), whereas preliminary studies were conducted at the Taiwan beamline BL12XU at SPring-8, Japan. HPCAT is supported by DOE-BES, DOE-NNSA, NSF, and the W.M. Keck Foundation. APS is supported by DOE-BES, under contract no. DE-AC02-06-CH11357. The work performed at BL12XU was partly supported by the NSC of Taiwan. The experiments in SPring-8 were performed under the approval with Japan Synchrotron Radiation Research Institute, Japan (proposal no. 2009B4252) and National Synchrotron Radiation Research Center, Taiwan (2008-2-087-5). Optical Raman and ruby fluorescence measurements at APS were performed at GSECARS with technical assists from I. Kantor and V. Prakapenka. J.F.L. and Z.M. acknowledge support from the U.S. National Science Foundation (EAR-0838221), Energy Frontier Research Centers (EFRCs), and the Carnegie/DOE Alliance Center (CDAC). S.D.J. acknowledges support from the U.S. National Science Foundation (EAR-0748707), the David and Lucile Packard Foundation, and CDAC. We thank G. Vankó for helpful discussions.

REFERENCES CITED

Akahama, Y. and Kawamura, H. (2007) Diamond anvil Raman gauge in multi-megabar pressure range. High Pressure Research, 27, 473–482.

Badro, J., Fiquet, G., Guyot, F., Rueff, J.P., Struzhkin, V.V., Vankó, G., and Monaco,

G. (2003) Iron partitioning in Earth's mantle: toward a deep lower mantle discontinuity. Science, 300, 789–791.

Badro, J., Rueff, J.P., Vankó, G., Monaco, G., Fiquet, G., and Guyot, F. (2004) Electronic transitions in perovskite: Possible nonconvecting layers in the lower mantle. Science, 305, 383–386.

Briois, V., Cartier dit Moulin, Ch., Sainctavit, Ph., Brouder, Ch., and Flan, A.-M. (1995) Full multiple scattering and crystal field multiplet calculations performed on the spin transition $Fe^{II}(phen)_2(NCS)_2$ complex at the iron K and $L_{2,3}$ X-ray absorption edges. Journal of the Americal Chemical Society, 117, 1019–1026.

Burns, R.G. (1985) Thermodynamic data from crystal field spectra. In S.W. Kieffer and A. Navrotsky, Eds., Microscopic to Macroscopic: Atomic environments to mineral thermodynamics, 14, p. 277–314. Reviews in Mineralogy, Mineralogical Society of America, Chantilly, Virginia.

——— (1993) Mineralogical Applications of Crystal Field Theory. Cambridge University Press, U.K.

Caliebe, W.A., Kao, C.-C., Hastings, J.B., Taguchi, M., Kotani, A., and de Groot, F.M.F. (1998) 1*s*2*p* resonant inelastic X-ray scattering in α-Fe_2O_3. Physical Review B, 58, 13452–13458.

Cartier dit Moulin, C., Rudolf, P., Flank, A.M., and Chen, C.T. (1992) Spin transition evidenced by soft X-ray absorption spectroscopy. Journal of Physical Chemistry, 96, 6196–6198.

Catalli, K., Shim, S.-H., Prakapenka, V.B., Zhao, J., Sturhahn, W., Chow, P., Xiao, Y., Liu, H., Cynn, H., and Evans, W.J. (2010) Spin state of ferric iron in $MgSiO_3$ perovskite and its effect on elastic properties. Earth and Planetary Science Letters, 289, 68–75.

Cressey, G., Henderson, C.M.B., and van der Laan, G. (1993) Use of L-edge X-ray absorption spectroscopy to characterize multiple valence states of 3d transition metals; a new probe for mineralogical and geochemical research. Physics and Chemistry of Minerals, 20, 111–119.

Gavriliuk, A.G., Lin, J.F., Lyubutin, I.S., and Struzhkin, V.V. (2006) Optimization of the conditions of synchrotron Mössbauer experiment for studying electron transitions at high pressures by the example of (Mg, Fe)O magnesiowüstite. Journal of Experimental and Theoretical Physics Letters, 84, 161–166.

Goncharov, A.F., Struzhkin, V.V., and Jacobsen, S.D. (2006) Reduced radiative conductivity of low-spin (Mg,Fe)O in the lower mantle. Science, 312, 1205–1208.

Griffith, J.S. (1961) The Theory of Transition Metal Ions, p. 466. Cambridge University Press, Cambridge, U.K.

Grocholski, B., Shim, S.-H., Sturhahn, W., Zhao, J., Xiao, Y., and Chow, C. (2009) Spin and valence states of iron in $(Mg_{0.8}Fe_{0.2})SiO_3$ perovskite. Geophysical Research Letters, 36, L24303.

Huse, N., Khalil, M., Kim, T.K., Smeigh, A.L., Jamula, L., McCusker, J.K., and Schoenlein, R.W. (2009) Probing reaction dynamics of transition-metal complexes in solution via time-resolved X-ray spectroscopy. Journal of Physics: Conference Series, 148, 012043.

Jackson, J.M., Sturhahn, W., Shen, G., Zhao, J., Hu, M.Y., Errandonea, D., Bass, J.D., and Fei, Y. (2005) A synchrotron Mössbauer spectroscopy study of (Mg,Fe) SiO_3 perovskite up to 120 GPa. American Mineralogist, 90, 199–205.

Jacobsen, S.D., Reichmann, H.J., Spetzler, H., Mackwell, S.J., Smyth, J.R., Angel, R.J., and McCammon, C.A. (2002) Structure and elasticity of single-crystal (Mg,Fe)O and a new method of generating shear waves for gigahertz ultrasonic interferometry. Journal of Geophysical Research, 107, 2037, DOI: 10.1029/2001JB000490.

Kantor, I.Y., Dubrovinsky, L.S., and McCammon, C.A. (2006) Spin crossover in (Mg,Fe)O: A Mössbauer effect study with an alternative interpretation of X-ray emission spectroscopy data. Physical Review B, 73, 100101.

Keppler, H., Kantor, I., and Dubrovinsky, L.S. (2007) Optical absorption spectra of ferropericlase to 84 GPa. American Mineralogist, 92, 433–436.

Lin, J.F. and Tsuchiya, T. (2008) Spin transition of iron in the Earth's lower mantle. Physics of the Earth and Planetary Interiors, 170, 248–259.

Lin, J.F., Struzhkin, V.V., Jacobsen, S.D., Hu, M., Chow, P., Kung, J., Liu, H., Mao, H.K., and Hemley, R.J. (2005) Spin transition of iron in magnesiowüstite in Earth's lower mantle. Nature, 436, 377–380.

Lin, J.F., Gavriliuk, A.G., Struzhkin, V.V., Jacobsen, S.D. Sturhahn, W., Hu, M., Chow, P., and Yoo, C.S. (2006) Pressure-induced electronic spin transition of iron in magnesiowüstite-(Mg,Fe)O. Physical Review B, 73, 113107.

Lin, J.F., Vankó, G., Jacobsen, S.D., Iota-Herbei, V., Struzhkin, V.V., Prakapenka, V.B., Kuznetsov, A., and Yoo, C.S. (2007) Spin transition zone in Earth's lower mantle. Science, 317, 1740–1743.

Lin, J.F., Watson, H.C., Vankó, G., Alp, E.E., Prakapenka, V.B., Dera, P., Struzhkin, V.V., Kubo, A., Zhao, J., McCammon, C., and Evans, W.J. (2008) Intermediate-spin ferrous iron in lowermost mantle post-perovskite and perovskite. Nature Geoscience, 1, 688–691, DOI: 10.1038/ngeo310.

Lin, J.F., Gavriliuk, A.G., Sturhahn, W., Jacobsen, S.D., Zhao, J., Lerche, M., and Hu, M. (2009) Synchrotron Mössbauer spectroscopic study of ferropericlase at high pressures and temperatures. American Mineralogist, 94, 594–599.

Lyubutin, I.S., Gavriliuk, A.G., Frolov, K.V., Lin, J.F., and Troyan, I.A. (2009) High-spin low-spin transition in $Mg_{0.75}Fe_{0.25}O$ magnesiowüstite at high pressures under hydrostatic conditions. Journal of Experimental and Theoretical Physics Letters, 90, 617–622.

Maddock, A.G. (1997) Mössbauer Spectroscopy: Principles and applications of the techniques, p. 258. Albion/Horwood Publishing, Chichester.

Mao, H.K., Bell, P.M., Shaner, J.W., and Steinberg, D.J. (1978) Specific volume measurements of Cu, Mo, Pd, and Ag and calibration of the ruby fluorescence pressure gauge from 0.06 to 1 Mbar. Journal of Applied Physics, 49, 3276–3283.

McCammon, C., Kantor, I., Narygina, O., Rouquette, J., Ponkratz, U., Sergueev, I., Mezouar, M., Prakapenka, V., and Dubrovinsky, L. (2008) Intermediate-spin ferrous iron in lower mantle perovskite. Nature Geoscience, 1, 684–687.

Narygina, O., Mattesini, M., Kantor, I., Pascarelli, S., Wu, X., Aquilanti, G., McCammon, C., and Dubrovinsky, L. (2009) High-pressure experimental and computational XANES studies of $(Mg,Fe)(Si,Al)O_3$ perovskite and (Mg,Fe)O ferropericlase as in the Earth's lower mantle. Physical Review B, 79, 174115.

Persson, K., Bengtson, A., Ceder, G., and Morgan, D. (2006) *Ab initio* study of the composition dependence of the pressure-induced spin transition in the $(Mg_{1-x}, Fe_x)O$ system. Geophysical Research Letters, 33, L16306.

Rueff, J.-P., Journel, L., Petit, P.-E., and Farges, F. (2004) Fe *K* pre-edges as revealed by resonant X-ray emission. Physical Review B, 69, 235107.

Speziale, S., Milner, A., Lee, V.E., Clark, S.M., Pasternak, M., and Jeanloz, R. (2005) Iron spin transition in Earth's mantle. Proceedings of the National Academy of Sciences, 102, 17918–17922.

Tsuchiya, T., Wentzcovitch, R.M., da Silva, C.R.S., and de Gironcoli, S. (2006) Spin transition in magnesiowüstite in Earth's lower mantle. Physical Review Letters, 96, 198501.

Westre, T.E., Kennepohl, P., DeWitt, J.G., Hedman, B., Hodgson, K.O., and Solomon, E.I. (1997) A multiplet analysis of Fe *K*-edge 1*s*→3*d* pre-edge features of iron complexes. Journal of American Chemical Society, 119, 6297–6314.

Wilke, M., Farges, F., Petit, P.-E., Brown, G.E., and Martin, F. (2001) Oxidation state and coordination of Fe in minerals: An Fe *K*-XANES spectroscopic study. American Mineralogist, 86, 714–730.

Vankó, G., Neisius, T., Molnar, G., Renz, F., Karpati, S., Shukla, A., and de Groot, F.M.F. (2006) Probing the 3*d* spin momentum with X-ray emission spectroscopy: The case of molecular-spin transitions. Journal of Physics and Chemistry B, 110, 11647–11653.

MANUSCRIPT RECEIVED JANUARY 9, 2010
MANUSCRIPT ACCEPTED APRIL 21, 2010
MANUSCRIPT HANDLED BY LARS EHM